



Scavenging malachite green dye from aqueous solutions using pomelo (*Citrus grandis*) peels: kinetic, equilibrium and thermodynamic studies

Olugbenga Solomon Bello^{a,b,*}, Mohd Azmier Ahmad^b, Banjo Semire^a

^aDepartment of P/A Chemistry, Ladoké Akintola University of Technology, P.M.B 4000, Ogbomoso, Oyo State, Nigeria, Tel. +2348035685435; email: osbello06@gmail.com (O.S. Bello), Tel. +2348038269809; email: semireban@yahoo.com (B. Semire)

^bSchool of Chemical Engineering, Engineering Campus, Universiti Sains Malaysia, 14300 Nibong Tebal, Penang, Malaysia, Tel. +60194700250; email: chazmier@eng.usm.my (M.A. Ahmad)

Received 13 December 2013; Accepted 12 June 2014

ABSTRACT

Activated carbon produced from pomelo peels (PPAC) was tested for its effectiveness in the removal of malachite green (MG) dye from aqueous solution. The PPAC prepared was characterized using TGA, BET, FTIR, SEM, pH_{pzc} , Elemental analysis and Boehm titration, respectively. The extent of dye adsorption was investigated as a function of pH, contact time, adsorbate concentration and solution temperature. Dye removal was pH dependent, resulting in 95.06% removal at pH 8.0. Quantum chemical studies suggested that the cationic MG dye possessed minimal molecular size at planar geometry coupled with high-electrostatic interaction thereby, enhancing the adsorption at high pH. Langmuir, Freundlich and Dubinin–Radushkevich (D–R) equilibrium isotherms were used to fit the adsorption data. Langmuir isotherm fit the adsorption data most with maximum monolayer adsorption capacity of 178.43 mg/g. The kinetic data fitted the pseudo-second-order model with correlation coefficient greater than 0.99. The mean free energy E (kJ/mol) got from the D–R isotherm indicated physisorption mechanism. Thermodynamic parameters; Gibbs free energy (ΔG°), enthalpy (ΔH°) and entropy (ΔS°) changes were also calculated, and the values indicated that the adsorption process was spontaneous and endothermic in nature. Regeneration efficiency of spent PPAC was studied using 0.2M HCl, the efficiency was found to be in the range of 92.71–96.35% after four cycles. The study showed that PPAC can be used as an effective, low cost and environmentally friendly adsorbent for the removal of MG dye from aqueous solution.

Keywords: Pomelo peel activated carbon; Malachite green; Adsorption isotherm; Kinetics; Quantum chemical studies

1. Introduction

Removal of toxic substances from water has been a challenge long-time ago; adsorption technique proved

best at minimizing this task [1,2]. Improper discharge of dyes from textiles, printing, dyeing, dyestuff manufacturing and food plants contributes to this menace thereby, causing significant threat to the ecosystem [3]. Malachite green (MG), tri-phenyl methane dye, has been widely used for dyeing of leather, wool and silk

*Corresponding author.

as well as in distilleries [4]. In addition, MG dye is also used as a fungicide and antiseptic in aquaculture industry to control fish parasites and diseases [5]. However, MG is very dangerous and highly cytotoxic to mammalian cells; it also acts as a liver tumour-enhancing agent. Dyes discharged into aquatic environment without proper treatment inhibits growth of aquatic animals and plants by blocking sunlight penetration [6,7]. Therefore, there is a need to treat these effluents prior to their discharge into receiving waters to prevent environmental pollution in aquatic ecosystems. Conventional wastewater treatment methods for removing dyes include physicochemical, chemical and biological methods, such as coagulation and flocculation [8], adsorption [9], ozonation [10], electrochemical techniques [11] and fungal decolonization [12]. Among these methods, adsorption has gained favour in recent years due to proven efficiency in the removal of pollutants from effluents. Activated carbon, as an adsorbent has been widely investigated for the adsorption of dyes [13], but its high cost limits its commercial application. Pomelo (*Citrus grandis*), the largest of citrus fruits, belongs to the family Rutaceae. Pomelo is native to southeastern Asia and Malaysia. In Malaysia, pomelo is widely grown in Perak, Kedah, Melaka, Kelantan and Johor states. This largest citrus fruit, growing as large as 30 cm in diameter and weighing as much as 10 kg; the rind is very thick but soft and easy to peel away. Pomelo (*Citrus grandis*) peel (PP) can be described as a new, low cost and abundantly available precursor. However, the usage of pomelo peel as an adsorbent is rather rare [14]. The thick peels of pomelo are candied or used as flavourings and marmalade. However, the enveloping membranous skin around the segments is bitter and usually discarded as waste.

Various adsorbent such as cocoa pod husks, mango peels, periwinkle shells, tin sulphide nanoparticle loaded on activated carbon, zinc oxide nanoparticle loaded on activated carbon and gold nanoparticles loaded on activated carbon have been evaluated for use in the removal of dyes from aqueous solution [15–22]. To the best of our knowledge, not much study has been reported on the beneficial use of pomelo peel. Therefore, this research was undertaken to examine the feasibility of pomelo peels, a lignocellulosic biomass for the preparation of activated carbon via carbonization and chemical activation. Structural, functional and elemental characterization of the prepared adsorbent was performed. The effects of initial MG dye concentration, solution temperature and pH on MG dye adsorption onto pomelo peel activated carbon (PPAC) were studied. Adsorption kinetics, isotherms and thermodynamic parameters were also evaluated and reported.

2. Materials and methods

2.1. Adsorbate

MG dye was supplied by Sigma–Aldrich (M) Sdn Bhd, Malaysia and used as received. MG has a chemical formula of $C_{52}H_{54}N_4O_{12}$, molecular weight of 927.00 g/mol and $\lambda_{max}=618$ nm. Stock solutions were prepared by dissolving accurately weighed samples of dye in deionized water.

2.2. Adsorbent preparation

Pomelo peel was washed and subsequently dried at 120°C overnight to remove the moisture content. It was cut into small pieces and then carbonized at 700°C under nitrogen flow (99.999%) for 1 h (first pyrolysis). A certain amount of produced char was then soaked with potassium hydroxide (KOH) at impregnation ratio of 1:1 (KOH pellets: char). The mixture was dehydrated in an oven overnight at 105°C; then pyrolyzed in a stainless steel vertical tubular reactor placed in a tube furnace under nitrogen flow of 150 cm³/min (second pyrolysis) to a final temperature of 800°C. Once the final temperature was reached, the gas flow was switched to CO₂ and activation was continued for 2 h. The sample was then cooled to room temperature under nitrogen flow and washed with 0.1 M HCl. It was further washed with deionized water until the pH of the washing solution reached 6.5–7.

2.3. Batch equilibrium studies

Batch equilibrium tests were carried out for adsorption of MG dye on PPAC. The effects of initial dye concentration, contact time, temperature and solution pH on the adsorption uptake were investigated. Sample solutions were withdrawn at equilibrium to determine residual concentrations. The solutions were filtered prior to analysis in order to minimize interference of the carbon fine with the analysis. For equilibrium studies, the experiment was carried out for 4 h to ensure that equilibrium was reached. The linear Beer–Lambert relationship between absorbance and concentration with the calibration curve was established by plotting the graph of absorbance vs. concentration of dye solutions. The concentration of MG dye solution before and after adsorption was determined using a double UV–vis spectrophotometer (UV-1800 Shimadzu, Japan) at a maximum wavelength of 618 nm. The amount of MG dye adsorbed at equilibrium, q_e (mg/g) was calculated according to Eq. (1):

$$q_e = \frac{(C_0 - C_e)V}{W} \quad (1)$$

where C_0 and C_e (mg/L) are the liquid-phase concentrations of MG dye at initial and at equilibrium, respectively. V (L) is the volume of the solution and W (g) is the mass of dry adsorbent used. For the batch kinetic studies, the same procedure was followed, but aqueous samples were taken at preset time intervals. The concentrations of MG dye were similarly measured. All experiments are conducted in triplicate, the mean values are reported.

2.4. Effect of initial MG dye concentration, contact time and solution temperature

One hundred millilitre of MG dye solution with initial concentrations of 50–400 mg/L was prepared in a series of 250-mL Erlenmeyer flasks. An equal mass of 0.20 g of the PPAC were added into each flask covered with glass stopper and the flasks were then placed in an isothermal water bath shaker (Model Protech, Malaysia) at temperature of 303 K with rotation speed of 120 rpm, until equilibrium point was reached. The effect of solution temperature on the MG dye adsorption process was examined by varying the adsorption temperature at 303, 318 and 333 K by adjusting the temperature controller of the water bath shaker. All experiments are conducted in triplicate, the mean values are reported.

2.5. Effect of solution pH

The effect of solution pH on the MG dye adsorption process was studied by varying the initial pH of solutions from 3 to 10. The pH was adjusted by adding 0.1 M hydrochloric acid and/or 0.1 M sodium hydroxide, and was measured using pH meter (Model Delta 320, Mettler Toledo, China). The MG dye initial concentration was fixed at 100 mg/L with adsorbent dosage of 0.2 g. The solution temperature was maintained at 303 K. Percentage dye removal was calculated using Eq. (2). All experiments are conducted in triplicate, the mean values are reported.

$$\text{Removal(\%)} = \frac{(C_0 - C_e)}{C_0} \times 100 \quad (2)$$

All experiments are conducted in triplicate, the mean values are reported.

2.6. Characterization of PPAC

Fourier transform infrared (FTIR) spectroscopic analysis was performed using FTIR spectroscope (FTIR-2000, Perkin Elmer). The spectra were measured from 4,000 to 400 cm^{-1} . The surface area, total pore volume and average pore diameter of the samples were determined from the adsorption isotherms of Nitrogen at 77 K using Micromeritics Model ASAP 2020 volumetric adsorption analyzer. Mesopore volume was calculated by subtracting total volume, obtained at a relative pressure of 0.99 from the micropore volume obtained from t -plot equation. The surface morphology of the samples was examined using a scanning electron microscope (Model VPFESEM Supra 35VP). Proximate analysis was carried out using thermo gravimetric analyzer (TGA) (Model Perkin Elmer TGA7, USA).

A series of 50 mL of 0.01 M NaCl solution was placed in a closed Erlenmeyer flask. The pH was adjusted to a value between 2 and 12 by adding 0.1 M HCl or 0.1 M NaOH solution. Then 0.15 g of each PPAC sample was added and agitated at 150 rpm for 48 h under atmospheric conditions. The final pH measured and the results were plotted with pH (Initial pH–Final pH) against final pH. The pH_{zpc} is the point where the curve pH_{final} vs. $\text{pH}_{\text{initial}}$ crosses the line $\text{pH}_{\text{initial}} = \text{pH}_{\text{final}}$ [23]. The total surface basicity and acidity of the samples were determined by titration with NaOH and HCl using Boehm titration method [24]. 0.15 g of PPAC was mixed with 50 mL of 0.05 N NaOH or HCl solutions for 48 h with continuous stirring. 10 mL of each filtrate was then titrated against 0.05 N HCl or NaOH, using phenolphthalein as indicator. Capacities for H^+ and OH^- were then measured. All experiments are conducted in triplicate, the mean values are reported.

3. Results and discussion

3.1. Characterization of PPAC

Results of proximate and ultimate analyses of PPAC are shown in Table 1. Result showed that moisture, ash and volatile matter contents are low; however, the fixed carbon content is satisfactory for MG dye adsorption. Ultimate analysis showed high percentage of elemental carbon, low hydrogen and nitrogen contents and an insignificant value for sulphur. Surface area is one of the most important properties of adsorbents. Table 2 presents the surface characteristics of PPAC. The surface area of PPAC was found to be 1357.21 m^2/g which was much higher than most conventional activated carbons such as, wood-based

Table 1
Proximate and ultimate analyses of PPAC

	Analysis	PPAC
Proximate (%)	Moisture	9.00
	Ash	8.20
	Volatile matter	11.40
	Fixed carbon	71.40
Ultimate (%)	Carbon	75.80
	Hydrogen	2.95
	Nitrogen	1.53
	Sulphur	0.32

Note: The analysis was carried out in triplicates; standard deviation of results is ± 0.002 .

activated carbon ($769 \text{ m}^2/\text{g}$) [25] and coal-based activated carbon ($331 \text{ m}^2/\text{g}$) [26]. The adsorbent pores were classified into three groups: micropore (diameter $< 2 \text{ nm}$), mesopore ($2\text{--}50 \text{ nm}$) and macropore ($> 50 \text{ nm}$) [27]. It can be seen from Fig. 1 that most pores of PPAC are in the mesopore range. The average pore diameter of the prepared sample was found to be 2.72 nm (Table 2) which further indicated that the activated carbon derived from pomelo peel was mesoporous. Activated carbon with D_p in mesopore range is suitable for both liquid- and gas-phase adsorption as well as electrochemical applications [27].

The FTIR spectra of PPAC before and after adsorption are shown in Fig. 2. The broad stretching absorption bands at $3,280\text{--}3,303 \text{ cm}^{-1}$, represents NH and bonded OH groups. There was a reduction in the intensity of these bands after dye adsorption indicating that these groups are involved in dye binding. The bands observed at $2,865$ and $2,932 \text{ cm}^{-1}$ are assigned to the symmetric and asymmetric stretching vibrations of the CH_3 and CH_2 groups and their bending vibrations are $1,371$ and $1,445 \text{ cm}^{-1}$ before and after MG dye adsorption. Carbonyl stretching band of un-ionized carboxylates in the adsorbent was observed at $1,740 \text{ cm}^{-1}$. The bands at $1,650$ and $1,540 \text{ cm}^{-1}$ corresponds to carbonyl stretching vibration of amide considered to be due to the combined effect of double

Table 2
Characteristics of PPAC

S_{BET} (m^2/g)	$S_{\text{ext.}}$ (m^2/g)	$S_{\text{ext.}}/S_{\text{BET}}$ (%)	$S_{\text{mic.}}$ (m^2/g)	$S_{\text{mic.}}/S_{\text{BET}}$ (%)	$V_{\text{tot.}}$ (cm^3/g)	$V_{\text{mic.}}$ (cm^3/g)	$V_{\text{mic.}}/V_{\text{tot.}}$ (%)	D_p nm
1357.41	922.42	67.07	452.16	32.87	1.61	0.33	20.32	2.72

Note: The analysis was carried out in triplicates; standard deviation of results is ± 0.002 .

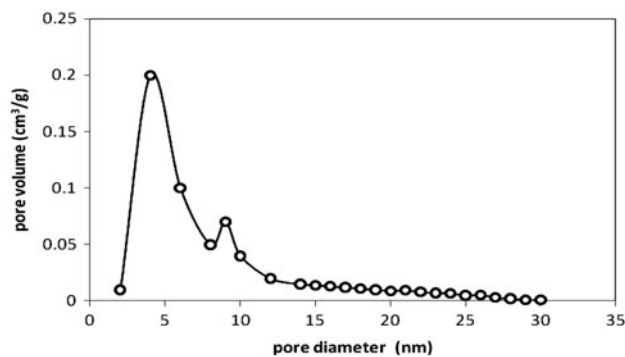


Fig. 1. Pore size distribution of PPAC.

bond stretching vibrations and NH deformation band before and after MG dye adsorption, respectively. Their intensities in the spectrum before dye adsorption decreases, while the NH deformation band shifts to $1,532 \text{ cm}^{-1}$ in the spectrum after MG dye adsorption onto PPAC. This behaviour reflects the interaction between the amino groups and dye ions. The band at $1,085 \text{ cm}^{-1}$ is due to $\text{C}=\text{O}$ stretching of carbonyl groups and the bending vibration of hydroxyl groups before adsorption, this band disappeared completely after MG dye adsorption indicating that this functional group is also involved in dye binding. Fig. 3 depicts the SEM image (magnification = $625\times$) of PPAC. It can be observed that the surface of PPAC contains well-developed pores in which there is a good possibility for MG dye to be adsorbed.

3.2. Effects of initial dye concentration and contact time

The effect of adsorption uptake on contact time at various MG concentrations at 303 K is shown in Fig. 4. The amount of MG dye adsorbed (mg/g) increased steadily with increase in contact time, at a point, the increase became gradual until equilibrium is reached. The amount of MG dye removed at equilibrium increased from 29.73 to $312.63 \text{ mg}/\text{g}$ with the increase in dye concentration from 50 to $400 \text{ mg}/\text{L}$ (Table 4). The extent of dye removal depends on the concentration of the dye. The initial dye concentration provides

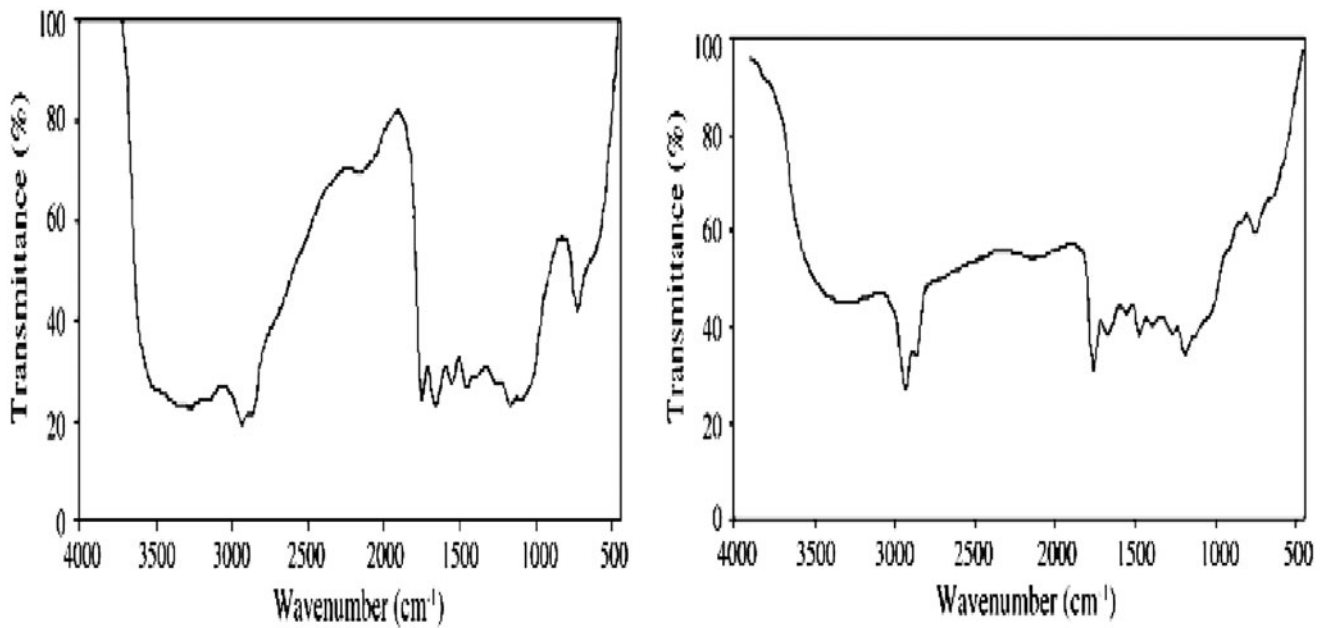


Fig. 2. FTIR spectra of PPAC (a) before MG dye adsorption and (b) after MG dye adsorption.

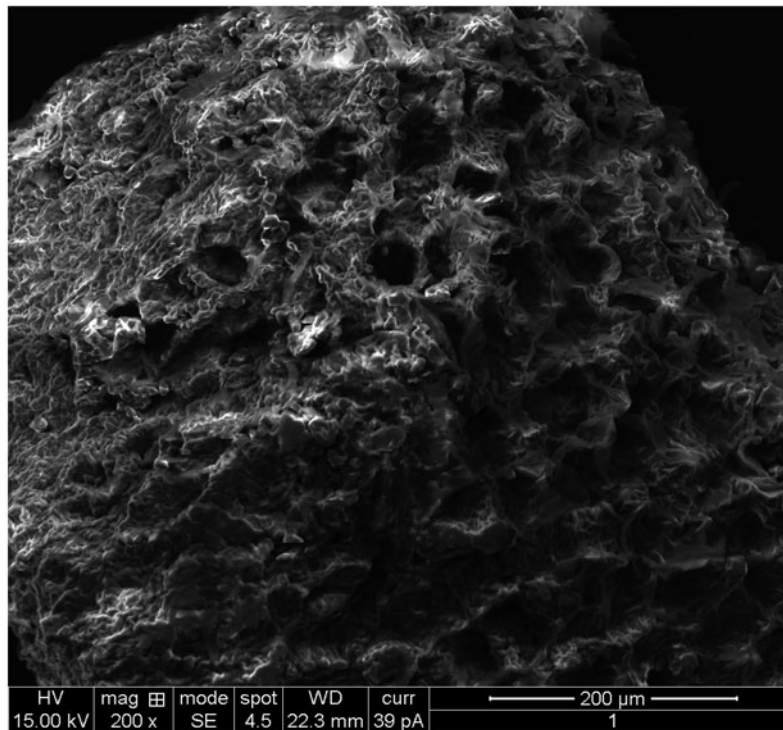


Fig. 3. SEM image of PPAC (magnification: 625×).

the necessary driving force to overcome the resistances to the mass transfer of MG dye between the aqueous and solid phases [28]. The effect of contact time was

also studied in order to find out the equilibrium time for maximum adsorption. Results show that equilibrium time required for the adsorption of MG onto

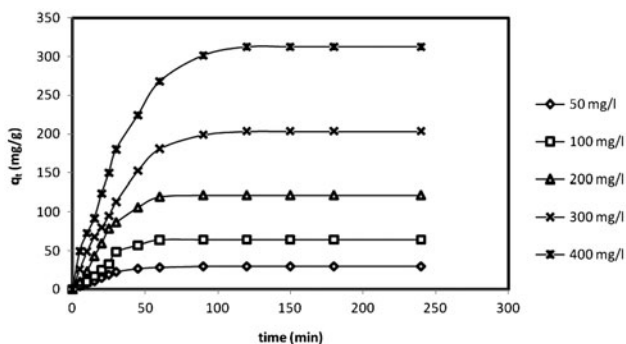


Fig. 4. Effect of initial concentration on the adsorption of MG dye by PPAC (Conditions: 0.2 g, adsorbent dosage, 120 rpm, 240 min agitation time and 303 K).

PPAC was 90 min for solutions with initial dye concentrations of 50–200 mg/L. However, equilibrium was attained in 120 min at 300–400 mg/L dye concentrations. In adsorption process, the dye molecules initially have to encounter the boundary layer effect before diffusing from the boundary layer film onto the adsorbent surface. Finally, the dye molecules have to diffuse into the porous structure of the adsorbent [29]. This theory explains the fact that due to the presence of large amount of dye molecules, it takes a relatively longer contact time to attain equilibrium at higher initial concentrations. The experiment was carried out for 240 min until equilibrium is reached.

3.3. Effect of temperature on dye adsorption

Temperature increase is known to increase the rate of diffusion of the adsorbate molecules across the external boundary layer and in the internal pores of the adsorbent particle, owing to the decrease in the viscosity of the solution. In addition, changing temperature will change the equilibrium capacity of the adsorbent for a particular adsorbate [30]. The adsorption capacity increased from 145.78 to 178.43 mg/g when temperature of the solution was increased from 303 to 333 K, indicating the process to be endothermic (Table 5). This is a result of increase in the mobility of MG dye as temperature increases. Interaction with active sites at the surface of the adsorbent increases as the dye molecules acquire sufficient energy thereby, producing a swelling effect within the internal structure of the PPAC facilitating penetration of more dye [31].

3.4. Effect of solution pH on percentage MG dye removal.

Generally, adsorption depends on pH and the zero point charge of the adsorbent (pH_{pzc}). The zero point

charge was found to occur at pH 7.5 meaning that PPAC surface has a positive charge in solution up to pH 7.5 and a negative charge above this pH (Fig. 5). Oxygen-containing functional groups are important characteristics of activated carbon because they determine the surface properties of such carbon and hence their quality as ion exchangers, adsorbents, catalysts and catalyst supports [32]. The contents of oxygen-containing functional groups with various acidic groups (carboxyl, lactonic and phenolic) as well as, the total amount of the basic groups are presented in Table 3. The content of basic groups is much higher than those of acidic groups. This is consistency with a value of pH_{pzc} 7.5 showing dominance of basic groups.

Fig. 6 shows the effect of pH on percentage MG dye adsorbed. The percentage of MG dye removed was low at pH range 3.0–6.0. Maximum adsorption was obtained at pH 8.0. The percentage of MG dye removal increased from 65.0 to 95.0% with an increase of pH from 6.0 to 8.0 and thereafter, removal became constant with a further increase of pH beyond 8.0. At lower pH, there was an increase

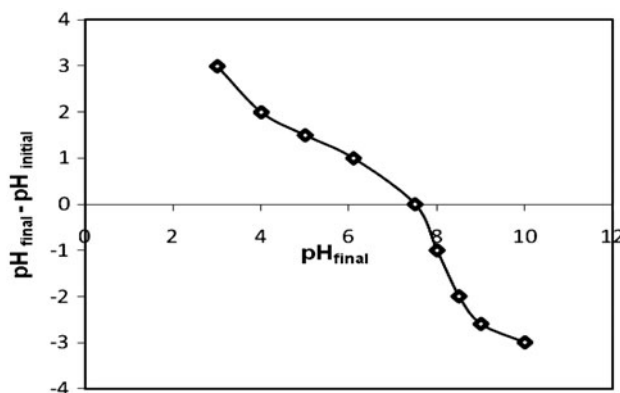


Fig. 5. The zeta potential vs. pH curve.

Table 3
Surface chemistry of PPAC

PPAC	Surface chemistry
Carboxylic (meq/g)	0.38
Lactonic (meq/g)	0.42
Phenolic (meq/g)	0.65
Acidic (meq/g)	1.44
Basic (meq/g)	4.36
pH_{pzc}	7.50

Note: The analysis was carried out in triplicates; standard deviation of results is ± 0.002 .

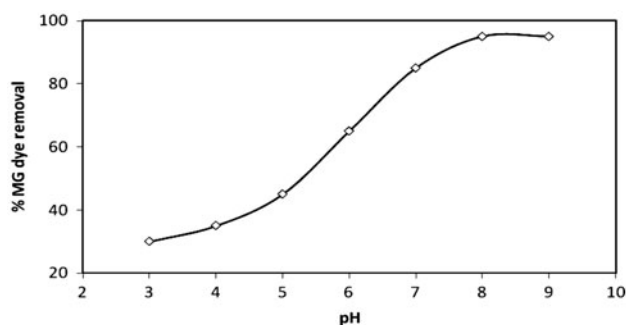


Fig. 6. Effect of pH on the adsorption of MG dye by PPAC (Conditions: 0.2 g adsorbent dosage, 120 rpm, 120 min agitation time, Temperature 303 K).

in H^+ in solution, causing the adsorbent surface to be positive; this resulted to strong electrostatic repulsion between positively charged adsorbent surface and positively charged MG dye cations hence, lesser percentage of MG dye molecule was adsorbed. However, as the pH increases, the charge of the solution becomes increasingly negative resulting in electrostatic attraction between the negatively charged adsorbent surface and positively charged MG dye cations leading to higher percentage of MG dye molecule adsorbed. A similar phenomenon was observed in the removal of MG dye from wastewater using hen feathers [33].

3.5. Adsorption kinetics

3.5.1. The pseudo-first-order kinetic model

The pseudo-first-order equation is generally expressed as follows [34]:

$$\ln(q_e - q_t) = \ln q_e - k_1 t \quad (3)$$

where q_e and q_t are the adsorption capacities at equilibrium and at time t , respectively (mg/g). k_1 is the rate constant for pseudo-first-order adsorption (/min). Plots of $\ln(q_e - q_t)$ against t at various dye concentrations resulted in graphs with negative slopes (Fig. not shown). k_1 and q_e are calculated from the slopes and intercepts, respectively. Although, the correlation coefficients (R^2) were high but comparison of the $q_{e,calc.}$ with the $q_{e,exp.}$, the values do not agree (Table 4). Therefore, the adsorption of MG dye onto PPAC does not follow the pseudo-first-order kinetics.

Table 4

A comparison of pseudo-first order, pseudo second-order and intra particle diffusion kinetic model rate constants calculated from experimental data at different concentrations

Models	C_o (mg/L)				
	50	100	200	300	400
Pseudo-first-order					
$q_{e,(exp)}$ (mg/g)	29.73	64.16	121.46	203.18	312.63
k_1 (/min)	0.16	0.25	0.36	0.40	0.48
$q_{e,(cal)}$ (mg/g)	16.18	49.45	106.73	181.43	281.19
R^2	0.92	0.95	0.95	0.98	0.98
Pseudo-second-order					
k_2 (g/mg/min)	0.52	0.49	0.42	0.35	0.317
$q_{e,(cal)}$ (mg/g)	30.85	65.98	122.89	204.49	314.87
R^2	0.99	0.99	0.99	0.99	0.99
Intraparticle diffusion					
k_{diff} (mg/g/min ^{1/2})	1.35	2.15	2.97	3.74	4.48
C	5.82	7.18	9.42	11.19	13.58
R^2	0.91	0.90	0.88	0.93	0.87

Note: The analysis was carried out in triplicates; standard deviation of results is ± 0.002 .

3.5.2. The pseudo-second-order kinetic model

The pseudo-second-order kinetic equation is expressed as [35]:

$$\frac{dq_t}{dt} = k_2(q_e - q_t)^2 \quad (4)$$

where k is the rate constant of pseudo-second-order adsorption (g/(mg min)). For the boundary conditions, $t=0$ to $t=t$ and $q_t=0$ to $q_t=q_t$, the integrated form of the equation becomes:

$$\frac{1}{q_e - q_t} = \frac{1}{q_e} + k_2 t \quad (5)$$

Rearranging this equation, we have a linear form:

$$\frac{t}{q_t} = \frac{1}{k_2 q_e^2} + \frac{1}{q_e} t \quad (6)$$

plots of t/q_t vs. t gave linear graphs from which q_e and k_2 were estimated from the slopes and intercepts of the plot (Fig. not shown) for various initial MG dye concentration. The R^2 values were as high as 0.99 and there were good agreement between $q_{e,calc.}$ and $q_{e,exp.}$ data obtained (Table 4). The good agreement shows

that the pseudo-second-order kinetic equation fits the adsorption data well.

3.5.3. Intraparticle diffusion model

The intraparticle diffusion equation is given as [36]:

$$q_t = k_{\text{diff}} t^{1/2} + C \quad (7)$$

where q_t is the amount of MG dye adsorbed (mg/g) at time t and k_{diff} (mg/g/min^{1/2}) is the rate constant for intraparticle diffusion. The values of q_t correlated linearly with values of $t^{1/2}$ and the rate constant k_{diff} directly evaluated from the slope of regression line (Table 4). The value of C gives an idea about the thickness of boundary layer, the larger the intercept the greater the boundary layer effect. From the plots of q_t against $t^{1/2}$ at various initial MG dye concentrations the plot was linear, but the plot did not pass through the origin (Fig. 7), suggesting that the adsorption process involved intraparticle diffusion, but that was not the only rate-controlling step. The intercepts (C) and the intraparticle rate constant values calculated from the slopes of the linear portions of the plots of Fig. 7 were presented in Table 4. Deviation of straight line from the origin indicates that the pore diffusion is not the sole rate-controlling step (Fig. 7). It could also be attributed to difference in rate of mass transfer in the initial and final stages of sorption. The k_{diff} and intercept, C values for all initial concentration were found to increase gradually (Table 4). Increase in dye concentration results in an increase in the driving force leading to increase in dye diffusion rate. The constant, C was found to increase with increase in initial dye concentration, indicating the boundary layer effect [37].

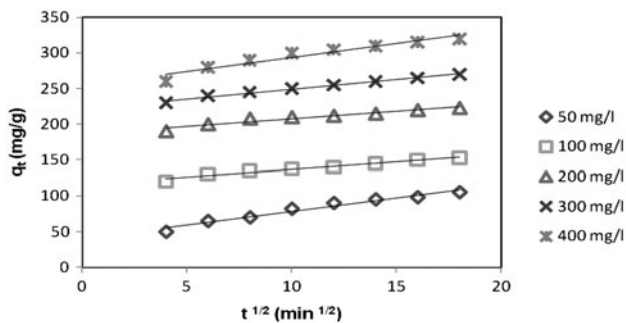


Fig. 7. Intra-particle diffusion plots for the adsorption of MG dye on PPAC at different initial dye concentrations. (Conditions: Temperature 303 K; 0.2 g adsorbent dosage, 120 rpm).

3.6. Adsorption isotherms

3.6.1. Langmuir isotherm model

The linearized form of Langmuir adsorption model is expressed as [38]:

$$\frac{C_e}{q_e} = \frac{C_e}{q_o} + \frac{1}{q_o K_L} \quad (8)$$

where C_e is the MG dye concentration in the solution at equilibrium (mg/L), q_e is the MG dye concentration on the adsorbent at equilibrium (mg/g), q_o is the monolayer adsorption capacity of adsorbent (mg/g) and K_L is the Langmuir adsorption constant (L/mg). A plot of C_e/q_e against C_e gave a straight line with a slope $1/q_o$ and an intercept of $1/q_o K_L$ (Fig. not shown). The R^2 values of Langmuir isotherm when compared with Freundlich isotherm indicate that the adsorption of the MG dye onto PPAC fits the Langmuir isotherm well. Values of q_o and K_L are calculated and reported in Table 5. To confirm the favourability of the adsorption process, the dimensionless equilibrium parameter (R_L) expressed by equation (9) was used:

$$R_L = \frac{1}{(1 + K_L C_o)} \quad (9)$$

Table 5

Isotherm constants and correlation coefficient for the adsorption of MG onto PPAC at different temperatures

Models	T (K)		
	303	318	333
Langmuir isotherm			
q_{max} (mg/g)	145.78	164.91	178.43
K_L (L/mg)	0.0056	0.0062	0.0068
R_L	0.15	0.13	0.12
R^2	0.99	0.99	0.99
Freundlich isotherm			
k_F	31.64	32.73	32.88
n	2.14	2.18	2.20
R^2	0.97	0.97	0.98
D-R isotherm			
q_o (mg/g)	63.41	62.72	61.97
β (mol ² k/J ²)	0.062	0.053	0.048
R^2	0.98	0.97	0.98
E_a (kJ/mol)	4.95	5.57	6.18

Note: The analysis was carried out in triplicates; standard deviation of results is ± 0.002 .

where C_o is the highest initial dye concentration in solution is used to confirm the favourability of the adsorption process that is ($0 < R_L < 1$) favourable, $R_L = 1$ linear, $R_L = 0$ irreversible or $R_L > 1$ unfavourable [38]. The values of R_L reported in Table 5 obtained at various temperatures were less than one, indicating that the adsorption of MG dye onto PPAC is favourable. The values of adsorption capacity obtained from Langmuir isotherm was compared with those from other adsorbents. PPAC proved to be a good adsorbent for the adsorption of MG dye from aqueous solutions (Table 6) [39–58].

3.6.2. Freundlich isotherm model

The linearized form of Freundlich model is expressed as [59]:

$$\log q_e = \frac{1}{n} \log C_e + \log k_f \quad (10)$$

where q_e is the amount of MG dye adsorbed at equilibrium (mg/g), C_e is the equilibrium concentration of the adsorbate (mg/L), k_f and n are constants incorporating the factors affecting the adsorption capacity

and the degree of non-linearity between the solute concentration in the solution and the amount adsorbed at equilibrium, respectively. Plots of $\log q_e$ vs. $\log C_e$ gave linear graphs (Fig. not shown) with high R^2 . Comparing the R^2 values with the ones obtained from Langmuir isotherms, the adsorption data do not fit the Freundlich isotherm well (Table 5). The values of k_f and n obtained from the slopes and intercepts of the graph are reported in Table 5. The value of n greater than one indicates that the adsorption is favourable.

3.6.3. Dubinin–Radushkevich isotherm model

The Dubinin–Radushkevich model (D–R model) [60], which does not assume a homogeneous surface or a constant sorption potential as the Langmuir model, is used to estimate the characteristic porosity of PPAC and the apparent energy of adsorption. It was also used to test the experimental data. It is expressed as:

$$\ln q_e = \ln q_o - \beta \varepsilon^2 \quad (11)$$

Table 6
Comparison of adsorption capacities of MG dye onto various adsorbents

Adsorbent	Capacity (mg/g)	Conditions		References
		pH	Temp (K)	
Carbon prepared from Borassus bark	20.70	6	303	[39]
<i>Caulerpa racemosa</i> var. <i>cylindracea</i> (marine alga)	25.67	6	318	[40]
<i>Saccharomyces cerevisiae</i>	17.00	5	308	[41]
Potato peel	32.39	4	298	[42]
Leaves of <i>Solanum tuberosum</i>	33.3	7	303	[43]
Unsaturated polyester Ce(IV) phosphate	1.01	8	300	[44]
Neem sawdust	4.35	7.2	303	[45]
Rubber wood sawdust	36.45	–	305	[46]
Commercial activated carbon	8.27	7	303	[47]
Waste fruit residues	37.03	5–8	300	[48]
Dried cashew nut bark carbon	20.09	6.60	–	[49]
Tamarind fruit shell	1.95	5	303	[50]
Epicarp of <i>Ricinus communis</i> activated carbon	27.78	–	–	[51]
<i>Annona squamosa</i> seed activated carbon	25.91	6	300	[52]
<i>Annona squamosa</i> seed	25.91	6	300	[53]
Cellulose powder	2.42	7.2	298	[54]
Kapok hull activated carbon	30.16	6.7	300	[55]
Chlorella-based biomass	18.4	7	298	[56]
Carbon prepared from <i>Arundo donax</i> root	8.69	5–7	303	[57]
Wood Apple shell	34.56	7.5	299	[58]
PPAC	178.43	8	333	<i>This work</i>

where β is the free energy of sorption per mole of the sorbate as it migrates to the surface of PPAC from an infinite distance in the solution ($\text{mol}^2 \text{k}/\text{J}^2$), q_e is the amount of adsorbate adsorbed at equilibrium, q_o is the maximum adsorption capacity and ε is the Polanyi potential (J/mol) that can be written as:

$$\varepsilon = RT \ln \left(1 + \frac{1}{C_e} \right) \quad (12)$$

where R and T are the gas constant (kJ/mol/K) and the absolute temperature (K), respectively. A plot of $\ln q_e$ vs. ε^2 gave a linear plot (Fig. not shown) where β and q_o are obtained from the slopes and intercepts, respectively (Table 5). Similarly, the β value obtained was then used to estimate the mean free energy of adsorption, E (Table 5).

$$E = \sqrt{\frac{1}{2\beta}} \quad (13)$$

The values of E were found to be between the ranges 4.95 and 6.18 kJ/mol over the range of temperatures used in this study. Since $E < 8$ kJ/mol, it suggests that the adsorption mechanism is physical in nature [61]. Similar results were obtained by other researchers [62,63].

3.7. Thermodynamic studies

Thermodynamic parameters; ΔG° , ΔH° and ΔS° were also determined to investigate the feasibility, spontaneity and the nature of the interaction. This was achieved using the equation:

$$\ln K_L = \frac{\Delta S^\circ}{R} - \frac{\Delta H^\circ}{RT} \quad (14)$$

$$\Delta G^\circ = -RT \ln K_L \quad (15)$$

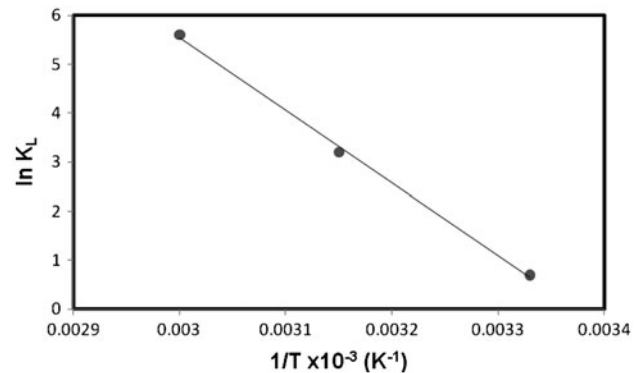


Fig. 8. Van't Hoff plot for adsorption of MG dye onto PPAC.

where K_L is the Langmuir constant, T is the temperature in K and R is the gas constant. A plot of $\ln K_L$ against $1/T$ gave linear plots (Fig. 8) from which ΔH° and ΔS° values were obtained from the slopes and intercepts, respectively. Thermodynamic parameters at various temperatures are reported in Table 7. The negative values of ΔG° indicate that the adsorption of MG dye onto PPAC is spontaneous and thermodynamically favoured. Moreover, when the temperature increases from 303 to 333 K, ΔG° changes from -21.55 to -24.22 kJ/mol, suggesting that adsorption is more spontaneous at higher temperature. The positive value of ΔH° (9.162 kJ/mol) indicates that the process is endothermic in nature, which is supported by the increase in the adsorption capacity of PPAC for MG dye with increasing temperature as observed from Table 5. Moreover, the positive value of ΔS° 0.146 kJ/mol/K suggests that there was increased randomness at the solid–liquid interface during the adsorption of MG dye onto PPAC.

3.8. Repeated adsorption–desorption studies

PPAC was subjected to adsorption–desorption cycles through regeneration step in between. It is observed from Table 8 that the efficiency of adsorption was retained only when PPAC after desorption was

Table 7
Thermodynamic parameters for the adsorption of MG onto PPAC at different Temperatures

Temp (K)	b (L/mol)	ΔG° (kJ/mol)	ΔH° (kJ/mol)	ΔS° (kJ/mol/K)
303	5191.20	−21.55	9.16	0.15
318	5747.40	−22.89		
333	6303.60	−24.22		

Note: The analysis was carried out in triplicates; standard deviation of results is ± 0.002 .

Table 8
Percentage adsorption of MG dye on regenerated PPAC

Dye	Adsorbent	Percentage MG dye desorbed				
		Repeated adsorption–desorption studies				
		Without HCl	With 0.2 M HCl			
		I cycle	II cycle	III cycle	IV cycle	
MG dye	PPAC	65.43	92.71	93.64	94.75	96.35

Note: The analysis was carried out in triplicates; standard deviation of results is ± 0.002 .

given a treatment with 0.2 M HCl solution. When the PPAC was reused without such treatment, there was a decrease in its adsorptive capacity.

3.9. Quantum chemical studies

Quantum chemical calculations were used to investigate the structural properties of MG in relation to its adsorption from aqueous solution. Thus, a theoretical study was undertaken to observe the possible physical

characters which could contribute to adsorption. In the present investigation, quantum chemical methods using semi-empirical and DFT were employed to explain the experimental results obtained in this study and to further give insight into the adsorption process of MG dye onto the PPAC surface. The parameters calculated are quantitative structure active relation, Mulliken charges, frontier molecular orbital (FMO) energies and stability of MG using DFT (B3LYP) method with 6–31G* basis set as implemented on

Table 9
Some selected geometrical and electronic parameters from quantum chemical calculations

Selected parameters	Neutral MG		Cationic MG	
	PM3	DFT/6–31G*	PM3	DFT/6–31G*
Total energy (au)	–	–1001.60	–	–1000.80
Heat of formation (kJ/mol)	284.75	–	996.50	–
HOMO (eV)	–8.31	–4.77	–10.92	–8.20
Solvation energy (kJ/mol)	–26.16	–19.03	–122.99	–116.74
LUMO (eV)	0.34	0.09	–5.25	–5.62
$E_{\text{HOMO}} - E_{\text{LUMO}}$ (eV)	8.65	4.86	5.67	2.58
Dipole moment (Debye)	0.77	1.81	2.12	3.07
Polarizability	70.28	71.32	70.81	71.51
PSA (\AA^2)	4.31	2.23	1.99	1.47
Log P	1.61	1.61	2.61	2.61
CPK (Area)	387.65	394.90	385.39	385.55
CPK (Volume)	381.54	383.31	379.39	379.06
Mulliken charges (<i>e</i>)				
N1	0.023	–0.47	0.12	–0.46
N2	0.023	–0.47	0.14	–0.46
C*	0.077	–0.34	0.33	0.02
Planarity (Dihedral angles, °)				
C12–C8–C22*–C1	–144.56	–145.82	–154.97	–152.24
C13–C8–C22*–C18	–90.55	–94.39	–156.42	–151.43
C2–C1–C22*–C18	–91.10	–102.24	–151.83	–151.38
C6–C1–C22*–C8	–144.81	–152.98	–153.11	–152.22
C14–C18–C22*–C1	–90.55	–103.17	–128.43	–137.18
C16–C18–C22*–C8	–144.81	–154.12	–128.27	–137.19

Notes: C* = central carbon atom of MG dye.

The analysis was carried out in triplicates; standard deviation of results is ± 0.002 .

SPARTAN 06. The neutral and cationic MG (since MG is a basic dye) was modelled for possible favourable structure of MG during adsorption. These calculated quantum chemical parameters were related to the adsorption efficiency of MG dye to provide information about the reactive behaviour of molecules.

The Mulliken charges, especially on the amino nitrogen N1/N2 and central carbon atom of MG are 0.023/0.023 and 0.077 for neutral MG and 0.116/0.143 and 0.333 e for cationic MG calculated at PM3. However, Mulliken charges calculated at DFT are $-0.472/-0.472$ and $-0.345e$ for neutral MG and $-0.464/-0.464$ and 0.015 e for cationic MG. The reactive ability of any molecule is considered to be closely related to their FMOs, the highest occupied molecular orbital (HOMO) and lowest unoccupied molecular orbital (LUMO). The HOMO is usually the region of high electron density in the molecule, which is often associated with the electron donating ability of that molecule to appropriate acceptor molecules with low-energy empty molecular orbital (LUMO), therefore, LUMO signifies the electron receiving tendency of a molecule. The HOMO and LUMO energies of the cationic MG dye are much lower than that of neutral MG, resulting in lower energy band gap; therefore, it

is expected that cationic MG should be more reactive in a basic medium (Table 9). This is supported by the LUMO map which is extended over nitrogen and the central carbon atoms in cationic MG providing more empty orbitals to accept electrons in the basic medium (Fig. 9(c) and (d)). The calculated solvation energy, dipole moment, polarizability and log P for cationic MG dye favour electrostatic interaction in basic medium; these are in agreement with the experimental observations that greater percentage of MG dye was adsorbed in a basic medium.

Another factor that contributed to the adsorption of dye molecules is the minimal molecular size at a planar geometry, this is important especially for effective adsorption onto adsorbent pores [64,65]. The geometries of both neutral and cationic MG dye revealed that cationic MG dye is more planar than that of neutral (Fig. 9), thereby facilitating higher adsorption of MG dye onto adsorbent spores in basic medium.

3.10. Cost estimation of PPAC

Accumulation of pomelo peel becomes an issue and contributes to serious environmental problems.

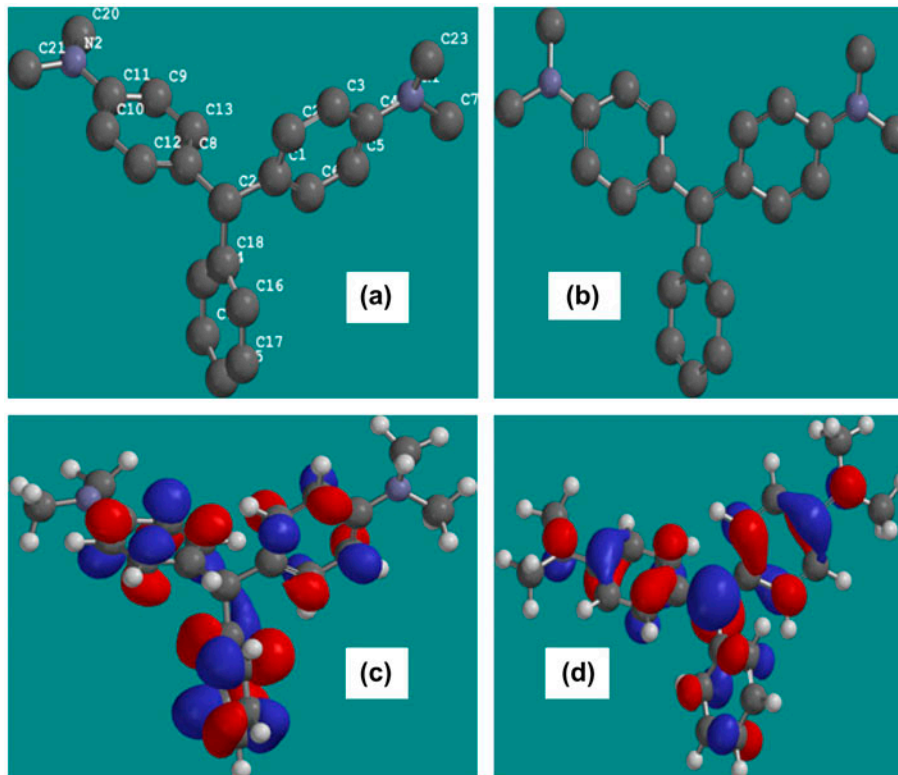


Fig. 9. Optimized structures and the LUMO maps of MG at B3LYP/6-31G*: (a) = neutral MG, (b) = cationic MG, (c) = LUMO map of neutral MG and (d) = LUMO map of cationic MG.

Hence, the utilization of such agricultural solid waste for wastewater treatment is most desirable. The cost of this waste as a dye adsorbent is only associated with the transport and process expenses which are approximately US\$ 50/ton whereas the average price of activated carbon used in Malaysia is US\$ 1,000–1,100/ton. Thus, the proposed PPAC adsorbent is over then 20 times cheaper than the commercially available activated carbon. Although the adsorption capacity of PPAC may be lower than commercial activated carbons, the adsorbent is a renewable material, abundantly available at little or no cost. PPAC promise to be an economical alternative to the expensive commercially available activated carbon in removal of basic dye from aqueous solutions.

4. Conclusion

PPAC was found to be one of the most promising adsorbents for the removal of MG dye from aqueous solutions: the amount of dye adsorbed increased steadily with increase in both the initial MG dye concentration and contact time. Equilibrium was reached at 90 and 120 min, respectively. Adsorption capacity increased with increase in temperature of the solution indicating an endothermic process. Maximum dye adsorption was obtained at pH 8.0. Quantum chemical studies also showed that LUMO map, dipole moment, energy band gap, solvation energy and the geometry of cationic MG molecule favour the adsorption of MG dye in basic medium. The kinetics of MG dye adsorption followed pseudo-second-order equation with $R^2 > 0.99$. The equilibrium data followed the linear Langmuir isotherm model most. Negative ΔG° values indicated that the adsorption of MG dye on PPAC was feasible and spontaneous. Positive value of ΔH° confirmed the endothermic nature of adsorption. The results indicated that PPAC can be used effectively for the removal of MG dye from aqueous solutions.

Acknowledgement

The corresponding author acknowledges the support obtained from Third World Academy of Science (TWAS) in form of grant; Research Grant number: 11-249 RG/CHE/AF/AC_1_UNESCO FR: 3240262674.

References

- [1] D.M. Ruthven, Principles of Adsorption and Desorption Processes, Wiley, New York, NY, 1984.
- [2] M. Suzuki (Ed.), Fundamentals of Adsorption IV, Kodansha, Tokyo, 1993.
- [3] A. Bhatnagar, A.K. Jain, A comparative adsorption study with different industrial wastes as adsorbents for the removal of cationic dyes from water, J. Colloid Interface Sci. 281 (2005) 49–55.
- [4] W. Cheng, S.-G. Wang, L. Lu, W.-X. Gong, X.-W. Liu, B.Y. Gao, H.-Y. Zhang, Removal of malachite green (MG) from aqueous solutions by native and heat treated anaerobic granular sludge, Biochem. Eng. J. 39 (2008) 538–546.
- [5] J. Zhang, Y. Li, C. Zhang, Y. Jing, Adsorption of malachite green from aqueous solution onto carbon prepared from *Arundo donax* root, J. Hazard. Mater. 150 (2008) 774–782.
- [6] Z. Bekçi, Y. Seki, L. Cavas, Removal of malachite green by using an invasive marine alga *Caulerpa racemosa* var. *cylindracea*, J. Hazard. Mater. 161 (2009) 1454–1460.
- [7] S.P. Raghuvanshi, R. Singh, C.P. Kaushik, Kinetics study of methylene blue dye bioadsorption on baggase, Appl. Ecol. Environ. Res. 2 (2004) 35–43.
- [8] R.P. Han, J.H. Zhang, W.H. Zou, J. Shi, H.M. Liu, Equilibrium biosorption isotherm for lead ion on chaff, J. Hazard. Mater. 125 (2005) 266–271.
- [9] V.K. Gupta, I. Ali, Suhas D. Mohan, Equilibrium uptake and sorption dynamics for the removal of a basic dye (basic red) using low cost adsorbents, J. Colloid Interface Sci. 265 (2003) 257–264.
- [10] Y.S. Ho, W.T. Chiu, C.C. Wang, Regression analysis for the sorption isotherms of basic dyes on sugarcane dust, Bioresour. Technol. 96 (2005) 1285–1291.
- [11] K.V. Kumar, Comparative analysis of linear and non-linear method of estimating the sorption isotherm parameters for malachite green onto activated carbon, J. Hazard. Mater. 136 (2006) 197–202.
- [12] Y.S. Ho, Second-order kinetic model for the sorption of cadmium onto tree fern: A comparison of linear and non-linear methods, Water Res. 40 (2006) 119–125.
- [13] R.P. Han, Y. Wang, W.H. Zou, Y.F. Wang, J. Shi, Comparison of linear and nonlinear analysis in estimating the Thomas model parameters for methylene blue adsorption onto natural zeolite in fixed-bed column, J. Hazard. Mater. 145 (2007) 331–335.
- [14] B.H. Hameed, D.K. Mahmoud, A.L. Ahmad, Sorption of basic dye from aqueous solution by pomelo (*Citrus grandis*) peel in a batch system, Colloids Surf., A 316 (2008) 78–84.
- [15] O.S. Bello, M.A. Ahmad, Adsorptive removal of a synthetic textile dye using cocoa pod husks, Toxicol. Environ. Chem. 93 (2011) 1298–1308.
- [16] O.S. Bello, M.A. Ahmad, Adsorption of dyes from aqueous solution using chemical activated mango peels, in: 2nd International Conference on Science and Technology (ICEST), vol. 2, 2011, pp. 108–109.
- [17] O.S. Bello, M.A. Ahmad, Response surface modeling and optimization of remazol brilliant blue reactive dye removal using periwinkle shell-based activated carbon, Sep. Sci. Technol. 46(15) (2011) 2367–2379.
- [18] O.S. Bello, M.A. Ahmad, Removal of remazol brilliant violet-5R dye using periwinkle shells, Chem. Ecol. 27 (5) (2011) 481–492.
- [19] M. Roosta, M. Ghaedi, A. Daneshfar, R. Sahraei, Experimental design based response surface methodology optimization of ultrasonic assisted adsorption of safarain O by tin sulfide nanoparticle loaded on activated carbon, Spectrochim. Acta, Part A 122 (2014) 223–231.

- [20] M. Ghaedi, A. Ansari, M.H. Habibi, A.R. Asghari, Removal of malachite green from aqueous solution by zinc oxide nanoparticle loaded on activated carbon: Kinetics and isotherm study, *J. Ind. Eng. Chem.* 20 (2014) 17–28.
- [21] M. Roosta, M. Ghaedi, A. Daneshfar, R. Sahraei, A. Asghari, Optimization of the ultrasonic assisted removal of methylene blue by gold nanoparticles loaded on activated carbon using experimental design methodology, *Ultra. Sonochem.* 21 (2014) 242–252.
- [22] M. Roosta, M. Ghaedi, N. Shokri, A. Daneshfar, R. Sahraei, A. Asghari, Optimization of the combined ultrasonic assisted/adsorption method for the removal of malachite green by gold nanoparticles loaded on activated carbon: Experimental design, *Spectrochim. Acta, Part A* 118 (2014) 55–65.
- [23] P. Nowicki, H. Wachowska, R. Pietrzak, Active carbons prepared by chemical activation of plum stones and their application in removal of NO₂, *J. Hazard. Mater.* 181 (2010) 1088–1094.
- [24] H.P. Boehm, Surface oxides on carbon and their analysis: A critical assessment, *Carbon* 40 (2002) 145–149.
- [25] M.A. Díaz-Díez, V. Gómez-Serrano, C. Fernández González, Porous texture of activated carbons prepared by phosphoric acid activation of woods, *J. Appl. Surf. Sci.* 238 (2004) 309–313.
- [26] E. Lorenc-Grabowska, G. Gryglewicz, Adsorption characteristics of congo red on coal-based mesoporous activated carbon, *Dyes Pigm.* 74 (2007) 34–40.
- [27] Z. Ryu, J. Zheng, M. Wang, B. Zhang, Characterization of pore size distributions on carbonaceous adsorbents by DFT, *Carbon* 37 (1999) 1257–1264.
- [28] V.C. Srivastava, M.M. Swamy, I.D. Mall, B. Prasad, I.M. Mishra, Adsorptive removal of phenol by bagasse fly ash and activated carbon: Equilibrium, kinetics and thermodynamics, *Colloids Surf., A* 272 (2006) 89–104.
- [29] O.S. Bello, T.T. Siang, M.A. Ahmad, Adsorption of remazol brilliant violet—5R reactive dye from aqueous solution by cocoa pod husk-based activated carbon: Kinetic, equilibrium and thermodynamic studies, *Asia-Pac. J. Chem. Eng.* 7 (2012) 378–388.
- [30] Z. Al-Qodah, Adsorption of dyes using shale oil ash, *Water Res.* 34 (2000) 4295–4303.
- [31] M. Alkan, M. Dogan, Adsorption kinetics of victoria blue onto perlite, *Fresen. Environ. Bull.* 12 (2003) 418–425.
- [32] T. Budinova, E. Ekinici, F. Yardim, A. Grimm, E. Björn-bom, V. Minkova, M. Goranova, Characterization and application of activated carbon produced by H₃PO₄ and water vapour activation, *Fuel Process. Technol.* 87 (2006) 899–905.
- [33] A. Mittal, Adsorption kinetics of removal of a toxic dye, malachite green, from wastewater by using hen feathers, *J. Hazard. Mater.* 133 (2006) 196–202.
- [34] S. Lagergren, B.K. Svenska, On the theory of so-called adsorption of materials, *Royal Swed. Acad. Sci. Doc.* 24 (1898) 1–13.
- [35] Y.S. Ho, G. McKay, Pseudo-second order model for sorption processes, *Process Biochem.* 34 (1999) 451–465.
- [36] W.J. Weber, J.C. Morris, Kinetics of adsorption on carbon from solution, *J. Sanit. Eng. Div. Am. Soc. Civil Eng.* 89 (1963) 31–59.
- [37] L. Wang, J. Zhang, R. Zhao, C. Li, Y. Li, C. Zhang, Adsorption of basic dyes on activated carbon prepared from *Polygonum orientale* Linn: Equilibrium, kinetic and thermodynamic studies, *Desalination* 254 (2010) 68–74.
- [38] I. Langmuir, The constitutional and fundamental properties of solids and liquids, *J. Am. Chem. Soc.* 38 (1916) 2221–2295.
- [39] S. Arivoli, M. Hema, P. Martin, D. Prasath, Adsorption of malachite green onto carbon prepared from borassus bark, *Arab. J. Sci. Eng.* 34 (2009) 31–36.
- [40] Z. Bekçi, Y. Seki, L. Cavas, Removal of malachite green by using an invasive marine alga *Caulerpa racemosa var. cylindracea*, *J. Hazard. Mater.* 161 (2009) 1454–1460.
- [41] P.T. Godbole, A.D. Sawant, Removal of malachite green from aqueous solutions using immobilized *Saccharomyces cerevisiae*, *J. Sci. Ind. Res.* 65 (2006) 440–442.
- [42] El-K. Guechi, O. Hamdaoui, Sorption of malachite green from aqueous solution by potato peel: Kinetics and equilibrium modeling using non-linear analysis method, *Arab. J. Chem.* 4(3) (2011) 243–360, doi: 10.1016/j.arabjc.2011.05.011.
- [43] N. Gupta, A.K. Kushwaha, M.C. Chattopadhyaya, Application of potato (*Solanum tuberosum*) plant wastes for the removal of methylene blue and malachite green dye from aqueous solution, *Arab. J. Chem.* 4(4) (2011) 361–490, doi: 10.1016/j.arabjc.2011.07.021.
- [44] A.A. Khan, R. Ahmad, A. Khan, P.K. Mondal, Preparation of unsaturated polyester Ce(IV) phosphate by plastic waste bottles and its application for removal of malachite green dye from water samples, *Arab. J. Chem.* 6 (2013) 361–368, doi: 10.1016/j.arabjc.2010.10.012.
- [45] S.D. Khattri, M.K. Singh, Removal of malachite green from dye wastewater using neem sawdust by adsorption, *J. Hazard. Mater.* 167 (2009) 1089–1094.
- [46] K. Vasanth Kumar, S. Sivanesan, Isotherms for malachite green onto rubber wood (*Hevea brasiliensis*) sawdust: Comparison of linear and non-linear methods, *Dyes Pigm.* 72 (2007) 124–129.
- [47] Indra Deo Mall, V.C. Srivastava, N.K. Agarwal, I.M. Mishra, Adsorptive removal of malachite green dye from aqueous solution by bagasse fly ash and activated carbon—Kinetic study and equilibrium isotherm analyses, *Colloids Surf., A* 264 (2005) 17–28.
- [48] P. Parimaladevi, V. Venkateswaran, Kinetics, thermodynamics and isotherm modeling of adsorption of triphenylmethane dyes (methyl violet, malachite green and magenta ii) on to fruit waste, *J. Appl. Technol. Environ. Sanit.* 1 (2011) 273–283.
- [49] S. Parthasarathy, N. Manju, M. Hema, S. Arivoli, Removal of malachite green from industrial wastewater by activated carbon prepared from cashew nut bark Alfa Universal, *Int. J. Chem.* 2 (2011) 41–46.
- [50] P. Saha, S. Chowdhury, S. Gupta, I. Kumar, R. Kumar, Assessment on the removal of malachite green using tamarind fruit shell as biosorbent, *Clean Soil Air Water* 38 (2010) 437–445.
- [51] T. Santhi, S. Manonmani, T. Smitha, Removal of malachite green from aqueous solution by activated carbon prepared from the epicarp of *Ricinus communis* by adsorption, *J. Hazard. Mater.* 179 (2010) 178–186.

- [52] T. Santhi, S. Manonmani, T. Smitha, Kinetics and isotherm studies on cationic dyes adsorption onto *Annona squamosa* seed activated carbon, *Int. J. Eng. Sci. Technol.* 2 (2010) 287–295.
- [53] T. Santhi, S. Manonmani, V.S. Vasantha, Y.T. Chang, A new alternative adsorbent for the removal of cationic dyes from aqueous solution, *Arab. J. Chem.* 4(3) (2011) 243–360, doi: [10.1016/j.arabjc.2011.06.004](https://doi.org/10.1016/j.arabjc.2011.06.004).
- [54] C. Pradeep Sekhar, S. Kalidhasan, V. Rajesh, N. Rajesh, Bio-polymer adsorbent for the removal of malachite green from aqueous solution, *Chemosphere* 77 (2009) 842–847.
- [55] S.P.S. Syed, Study of the removal of malachite green from aqueous solution by using solid agricultural waste, *Res. J. Chem. Sci.* 1 (2011) 88–93.
- [56] W.T. Tsai, H.R. Chen, Removal of malachite green from aqueous solution using low-cost chlorella-based biomass, *J. Hazard. Mater.* 175 (2010) 844–849.
- [57] J. Zhang, Y. Li, C. Zhang, Y. Jing, Adsorption of malachite green from aqueous solution onto carbon prepared from *Arundo donax* root, *J. Hazard. Mater.* 150 (2008) 774–782.
- [58] A.S. Sartape, A.M. Mandhare, V.V. Jadhav, P.D. Raut, M.A. Anuse, S.S. Kolekar, Removal of malachite green dye from aqueous solution with adsorption technique using *Limonia acidissima* (wood apple) shell as low cost adsorbent, *Arab. J. Chem.* 7(1) (2014) 1–17, doi: [10.1016/j.arabjc.2013.12.019](https://doi.org/10.1016/j.arabjc.2013.12.019).
- [59] H.M.F. Freundlich, Over the adsorption in solution, *Z. Phys. Chem.* 57 (1906) 385–470.
- [60] M.M. Dubinin, L.V. Radushkevich, Proceedings of the academy sciences, *Phys. Chem. Sec. USSR* 55 (1947) 331–333.
- [61] F. Helfferich, *Ion-exchange*, McGraw-Hill Book Co-education, New York, NY, 1962.
- [62] S. Arivoli, M. Thenkuzhali, Kinetic, mechanistic, thermodynamic and equilibrium studies on the adsorption of rhodamine B by acid activated low cost carbon, *Elec. J. Chem.* 5 (2008) 187–200.
- [63] V.B.H. Dang, H.D. Doan, T. Dang-Vu, A. Lohi, Equilibrium and kinetics of biosorption of cadmium(II) and copper(II) ions by wheat straw, *Bioresour. Technol.* 100 (2009) 211–219.
- [64] R.S. Susan, V.M. Gunko, O.M. Bakalinska, C.A. Howell, Y.Z.M.T. Kartel, G.J. Phillips, S.V. Mikhailovsky, Adsorption of anionic and cationic dyes by activated carbons, PVA hydrogels, and PVA/AC composite, *J. Colloid Interface Sci.* 358 (2011) 582–592.
- [65] O.S. Bello, Semire Banjo, Equilibrium, kinetic, and quantum chemical studies on the adsorption of congo red using *Imperata cylindrica* leaf powder activated carbon, *Toxicol. Environ. Chem.* 94 (2012) 1114–1124.